Guest Gas Enclathration in Semiclathrates of Tetra-n-butylammonium Bromide: Stability Condition and Spectroscopic Analysis

ARTICLE *in* LANGMUIR · JULY 2011

Impact Factor: 4.46 · DOI: 10.1021/la202143t · Source: PubMed

6 AUTHORS, INCLUDING:

Jaehyoung Lee
Korean Institute of Geoscience and Mineral…
29 PUBLICATIONS **329** CITATIONS
SEE PROFILE

Yongwon Seo
Ulsan National Institute of Science and Tech…
55 PUBLICATIONS **1,062** CITATIONS
SEE PROFILE

Langmuir

ARTICLE

pubs.acs.org/Langmuir

Guest Gas Enclathration in Semiclathrates of Tetra-*n*-butylammonium Bromide: Stability Condition and Spectroscopic Analysis

Seungmin Lee,[†] Sungmin Park,[†] Youngjun Lee,[†] Jaehyoung Lee,[‡] Huen Lee,[⊥] and Yongwon Seo*,[†]

[†]Department of Chemical Engineering, Changwon National University, Gyeongnam 641-773, Republic of Korea

[‡]Petroleum & Marine Resources Division, Korea Institute of Geoscience & Mineral Resources (KIGAM), Daejeon 305-350, Republic of Korea

[⊥]Department of Chemical and Biomolecular Engineering, Korea Advanced Institute of Science and Technology (KAIST), Daejeon 305-701, Republic of Korea

Supporting Information

ABSTRACT: In this study, guest gas enclathration behavior in semiclathrates of tetra-*n*-butylammonium bromide (TBAB) was closely investigated through phase equilibrium measurement and spectroscopic analysis. The three-phase equilibria of semiclathrate (H), liquid water (L_W), and vapor (V) for the ternary CH_4 + TBAB + water and CO_2 + TBAB + water mixtures with various TBAB concentrations were experimentally measured to determine the stability conditions of the double TBAB semiclathrates. Equilibrium dissociation temperatures for pure TBAB semiclathrate were also measured at the same concentrations under atmospheric conditions. The dissociation temperature and dissociation enthalpy of pure TBAB semiclathrate were confirmed by differential scanning calorimetry. The experimental results showed that the double CH_4 (or CO_2) + TBAB semiclathrates yielded greatly enhanced thermal stability when compared with pure CH_4 (or CO_2) hydrate. The highest stabilization effect was observed at the stoichiometric concentration of pure TBAB semiclathrate, which is 3.7 mol %. From the NMR and Raman spectroscopic studies, it was found that the guest gases (CH_4 and CO_2) were enclathrated in the double semiclathrates. In particular, from the cage-dependent ^{13}C NMR chemical shift, it was confirmed that CH_4 molecules were captured in the 5^{12} cages of the double semiclathrates.

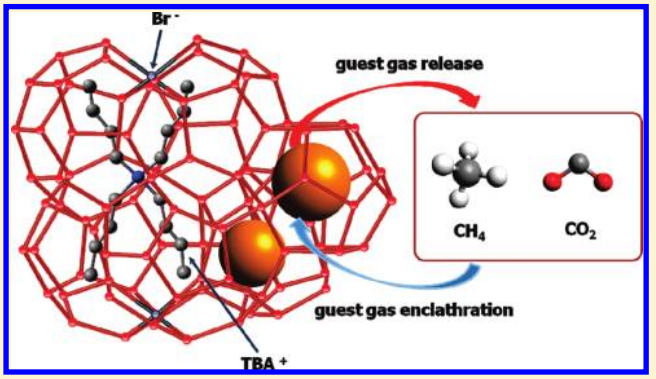

INTRODUCTION

Gas hydrates are nonstoichiometric crystalline compounds formed when "guest" molecules of suitable size and shape are incorporated into the well-defined cages in the "host" lattice made up of hydrogen-bonded water molecules.[1] In gas hydrates, guest molecules that are captured in the cages interact with water molecules through van der Waals forces.[1] Tetra-*n*-butylammonium bromide (TBAB) forms semiclathrates with water molecules at atmospheric pressure. In TBAB semiclathrates, anions such as Br^- form cage structures with water molecules and the tetra-*n*-butylammonium cations (TBA^+) occupy four partially broken cages.[2−5] Semiclathrates have many physical and structural properties in common with gas hydrates. The main difference is that, in gas hydrates, the guest molecules are not physically bonded to water lattices, while in semiclathrates, guest molecules can both form part of the host lattice and occupy cages after breaking part of the cage structure.[1−5] Because empty cages of TBAB semiclathrates can capture small-sized gas molecules at mild conditions, TBAB semiclathrates have attracted great attention as a new gas storage and separation material. Chapoy et al.[6] and Hashimoto et al.[7,8] suggested that TBAB semiclathrates could be a potential hydrogen storage medium because hydrogen (H_2) can be enclathrated in the TBAB semiclathrates at much lower pressure conditions. Kamata et al.[9] showed that small gas molecules such as methane (CH_4) and hydrogen sulfide (H_2S) were selectively occupied in dodecahedral cages of TBAB semiclathrates, whereas larger gas molecules such as ethane (C_2H_6) and propane (C_3H_8) were not incorporated into the TBAB semiclathrates. Duc et al.[10] and Fan et al.[11] used TBAB as a thermodynamic promoter that can provide remarkable pressure reduction for gas hydrate formation in the application to the process for capturing carbon dioxide (CO_2) from flue and fuel gas mixtures.

The phase equilibria of the double semiclathrates of TBAB + guest gases are essential in designing a gas storage and separation process because the phase equilibrium is closely related to the formation/dissociation conditions and stability region of the double semiclathrates. The guest gas enclathration behavior in

Received: March 16, 2011
Revised: July 11, 2011
Published: July 12, 2011

the double semiclathrates is also very useful in estimating the storage capacity and preferential occupation of guest gas and in predicting the structure transition of semiclathrates according to TBAB concentrations. Even though a few studies have covered the semiclathrate phase equilibria for guest gases in the presence of TBAB and some limited results of Raman spectroscopic analysis on the pure and double TBAB semiclathrates have been reported,[7,8,12−16] more systematic approaches based on thermodynamic and spectroscopic viewpoints should be adopted to verify the feasibility of the gas storage and separation process using TBAB semiclathrates.

Therefore, we attempted to closely investigate semiclathrate phase equilibria and guest gas enclathration behavior for CH_4 and CO_2 in the presence of TBAB. CH_4 and CO_2 are small enough to be captured in the empty cages of TBAB semiclathrates and are industrially important guest gases for the gas hydrate application process because CH_4 is a major component of natural gas and CO_2 is a target guest of flue and fuel gas mixtures. First, the dissociation temperatures of pure TBAB semiclathrates under atmospheric pressure conditions were measured at three different concentrations of TBAB. Differential scanning calorimetry (DSC) was also used to confirm the dissociation temperature and dissociation enthalpy of pure TBAB semiclathrate. Second, the three-phase equilibria (semiclathrate (H)−liquid water (L_W)−vapor (V)) for the ternary CH_4 + TBAB + water and CO_2 + TBAB + water mixtures at three different concentrations of TBAB were experimentally measured to determine the stability conditions of the double TBAB semiclathrates. Furthermore, the pure and double semiclathrates were analyzed via NMR and Raman spectroscopy to examine the structure details and guest gas enclathration.

EXPERIMENTAL SECTION

Semiclathrate Phase Equilibria. The CH_4 and CO_2 gases used for the present study were supplied by Union Gas (Republic of Korea) and had stated purities of 99.95% and 99.99%, respectively. TBAB with a purity of 99% and THF with a purity of 99.9% were purchased from Sigma-Aldrich, St. Louis, MO. Doubly distilled deinonized water was used. All materials were used without further purification.

A schematic diagram of the experimental apparatus used in this study is shown in previous papers.[17−19] The experimental apparatus for the clathrate phase equilibria was specially designed to accurately measure the clathrate dissociation pressures and temperatures. The equilibrium cell was made of 316 stainless steel and had an internal volume of about 200 cm^3. Two sapphire windows equipped in the front and back of the cell allowed the visual observation of phase transitions that occurred inside the equilibrium cell. The cell content was vigorously agitated by an impeller-type stirrer. A thermocouple with an accuracy of ±0.1 K for full ranges was inserted into the cell to measure the inner content. This thermocouple was calibrated using an ASTM 63C mercury thermometer (Ever Ready Thermometer) with a resolution of ±0.1 K. A pressure transducer (VPRT, Valcom, Japan) with an uncertainty of 0.02 MPa was used to measure cell pressure. The pressure transducer was also calibrated using a Heise Bourdon tube pressure gauge (CMM-137219, 0−10 MPa range) having a maximum error of ±0.01 MPa in the full range.

The experiment for clathrate phase equilibrium measurements began with charging the equilibrium cell with about 80 cm^3 of TBAB solution. Before each experimental run, the equilibrium cell was flushed at least three times with the clathrate-forming gas to remove any residual air. After the equilibrium cell was pressurized to the desired pressure with CH_4 or CO_2, the whole main system was slowly cooled to a temperature lower than the expected equilibrium temperature. Due to thermal contraction, the cell pressure was slightly decreased by decreasing the temperature at a cooling rate of 1 K/h. Then an abrupt pressure depression was observed at the stage of clathrate crystal growth after nucleation. When the pressure depression due to clathrate formation reached a steady-state condition, the temperature was increased in 0.1 K steps with sufficient time, and accordingly, the cell pressure was increased with clathrate dissociation. After all the clathrates were dissociated with increasing temperature, the cell pressure was again slightly increased due to thermal expansion. The H−L_W−V equilibrium points at each pressure condition were determined from the intersection between the clathrate dissociation and thermal expansion lines. For pure TBAB semiclathrates, the dissociation equilibrium temperature under atmospheric pressure conditions was determined by visual observation in a transparent flask with a cap. The content was vigorously agitated by a magnetic spin bar with an external magnet immersed in a water bath. The system temperature was raised in 0.1 K steps with sufficient time after completion of semiclathrate formation. The temperature at which a very small amount of crystals disappeared was considered as an equilibrium dissociation point at a given TBAB concentration under atmospheric pressure conditions. For both double and pure semiclathate systems, the measurement at each data point was repeated more than two times, and the average value with the measurement error is presented in this study.

Confirmation of the dissociation temperature and dissociation enthalpy of pure TBAB semiclathrate was conducted by DSC (Q10, TA Instruments, New Castle, DE). A TBAB solution of about 3.5×10^{-3} cm^3 was sealed in an aluminum pan and placed in the DSC cell. The sample was cooled to 243 K at a rate of 1 K/min, and semiclathrate was formed while the sample cooled. Then the sample was heated to 303 K at a rate of 1 K/min to dissociate the semiclathrate. The area for the phase transition peak corresponds to the heat absorbed due to dissociation.

NMR and Raman Analysis. The hydrate and semiclathrate samples for NMR and Raman analysis were prepared in the same apparatus as that used for measuring semiclathrate phase equilibria. To avoid any coexistence of pure CH_4 (or CO_2) hydrate and double semiclathrates, all the NMR and Raman samples of the double CH_4 (or CO_2) + TBAB semiclathrates were prepared at pressure and temperature conditions where CH_4 (or CO_2) molecules are unable to form structure I gas hydrate. For the analysis of the pure TBAB and double CH_4 + TBAB semiclathrates, a Bruker 400 MHz solid-state NMR spectrometer that belongs to the Korea Basic Science Institute (KBSI) was used in this study. The NMR spectra were recorded at 243 K and atmospheric pressure by placing the semiclathrate samples within a 4 mm o.d. Zr rotor that was loaded into the variable-temperature (VT) probe. The temperature of the probe was maintained at 243 K during measurement by controlling the flow rate of the liquid N_2 vapor. All ^{13}C NMR spectra were recorded at a Larmor frequency of 100.6 MHz with magic angle spinning (MAS) at about 2−4 kHz. A pulse length of 2 μs and pulse repetition delay of 10 s under proton decoupling were employed when the radio frequency field strengths of 50 kHz corresponding to 5 μs 90° pulses were used. The downfield carbon resonance peak of adamantane, assigned a chemical shift of 38.3 ppm at 300 K, was used as an external chemical shift reference.

For the Raman spectra of the pure CO_2 hydrate, mixed CO_2 + THF hydrate, and double CO_2 + TBAB semiclathrates, the formed hydrates or semiclathrates were finely powered in the liquid N_2 vessel and pelletized into a cylindrical type (1 cm diameter and 0.5 cm height). Under atmospheric pressure conditions, Raman spectra were obtained using a JASCO NRS-3100 Raman spectrometer (Japan) with a thermoelectrically cooled CCD detector and 1800 grooves/mm holographic grating. The excitation source was a diode-pumped solid-state laser emitting a 532 nm line, and the laser intensity was typically 7 mW. The temperature of the sample was maintained at approximately 170 K during measurement by controlling the flow rate of the liquid N_2 vapor.

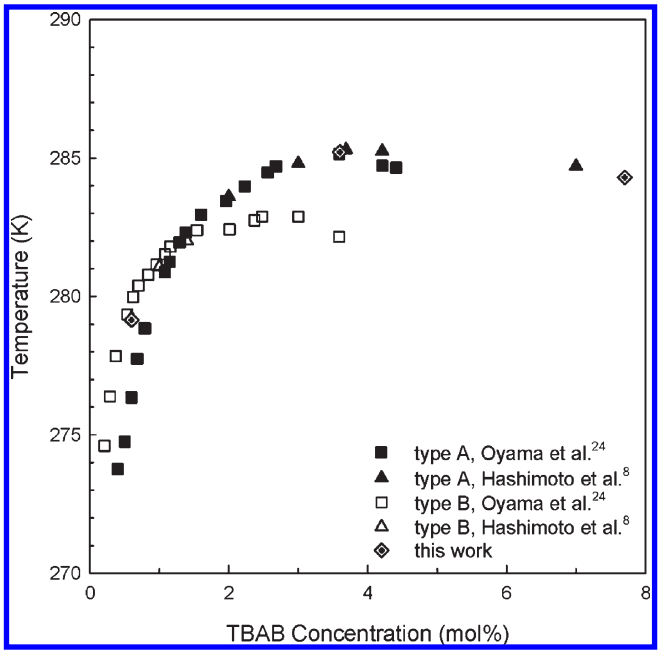

Figure 1. Phase diagram of the TBAB semiclathrate under atmospheric pressure conditions.

A more detailed description of NMR and Raman analysis is given in previous papers.[20−22]

RESULTS AND DISCUSSION

Lipkowski et al.[23] and Aladko et al.[4] reported that TBAB forms semiclathrates with stoichiometries of TBAB·24H_2O, TBAB·26H_2O, TBAB·32H_2O, and TBAB·36H_2O, which correspond to different crystal structures. On the other hand, Shimada et al.[5] and Oyama et al.[24] reported that TBAB semiclathrate has two different crystal structures, type A (TBAB·26H_2O) and type B (TBAB·38H_2O), which have different transmittances, refractions, and crystal morphologies, depending on the TBAB concentration of aqueous solution. In the region of concentration lower than 1.4 mol %, type B semiclathrate forms preferentially, while type A semiclathrate is more stable in the region of concentration higher than 1.4 mol %. In the present study, the dissociation temperature of pure TBAB semiclathrates was measured at TBAB concentrations of 0.6, 3.7, and 7.7 mol % under atmospheric pressure conditions. The phase equilibrium relation of temperature−composition for the pure TBAB semiclathrate system is shown in Figure 1. The equilibrium data measured in this study were in good agreement with the literature values.[7,24] As shown in Figure 1, TBAB semiclathrate is most stable at the stoichiometric concentration (3.7 mol %) of type A TBAB semiclathrate, where the equilibrium temperature is 285.25 ± 0.05 K and the hydration number is TBAB·26H_2O.

The dissociation temperature of pure TBAB semiclathrate was also confirmed through DSC. Figure 2 shows the dissociation process of TBAB semiclathrate in DSC under atmospheric pressure conditions. The onset temperature of the endothermic peak is taken as the dissociation temperature.[25] The resulting dissociation temperature for pure TBAB semiclathrate of 3.7 mol % was 285.05 ± 0.05 K, which is very close to the value (284.8 K) presented by Deschamps and Dalmazzone[26] using DSC and the value (285.25 K) obtained in the conventional reactor used in this study. For semiclathrate with 3.7 mol % TBAB, it was found from the heat flow of DSC that there was only one endothermic peak, indicating that only type A TBAB semiclathrate was formed without an ice peak. The heat of dissociation for type A TBAB semiclathrate was found to be 193 J/g, which is also quite similar to the literature value.[24]

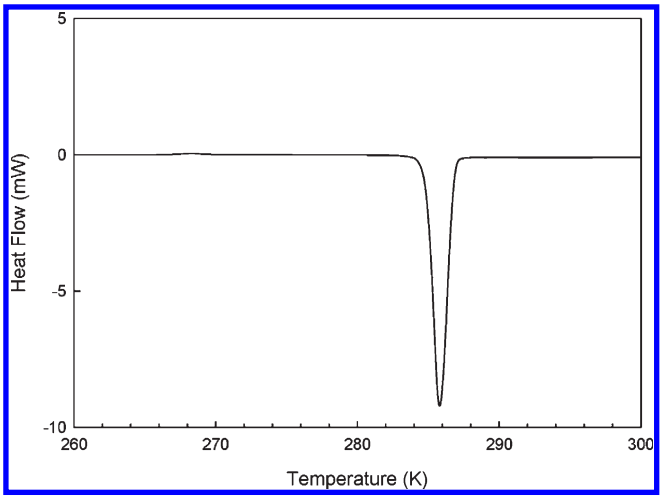

Figure 2. Dissociation process of TBAB semiclathrate in DSC under atmospheric pressure conditions.

The three-phase equilibria (H−L_W−V) for the CH_4 + TBAB + water systems were measured to determine the stability conditions of the CH_4 + TBAB semiclathrates at three different TBAB concentrations of 0.6, 3.7, and 7.7 mol %, and the overall results are summarized in Table 1 and shown in Figure 3 along with the three-phase equilibrium data of the pure CH_4 hydrate.[27] The presence of TBAB led to the promotion of clathrate stability, which means that hydrate dissociation occurs at a lower pressure for any given temperature or at a higher temperature for any given pressure when compared with that of a pure CH_4 hydrate system. The CH_4 + TBAB semiclathrates were more stabilized when the TBAB concentration increased from 0.6 to 3.7 mol %. However, at 7.7 mol %, the stabilization effect for the CH_4 + TBAB semiclathrate was less than that at 3.7 mol %. As can be expected from the phase diagram of the pure TBAB semiclathrate in Figure 1, the maximum stabilization effect of TBAB was observed at 3.7 mol %, which corresponds to the stoichiometric concentration of type A TBAB semiclathrate (TBAB·26H_2O). At 7.7 mol %, the stoichiometric amount of TBAB participates in forming the TBAB semiclathrate with CH_4; however, the excess amount of TBAB remains as free ions of TBA^+ and Br^-, resulting not in action as a semiclathrate former but action as an inhibitor. Therefore, at a specified temperature, the semiclathrate equilibrium pressure at 7.7 mol % was higher than that at 3.7 mol %.

The phase equilibria for CO_2 + TBAB + water systems showed almost the same trend as those for CH_4 + TBAB + water systems, as shown in Figure 4 and Table 2. The presence of TBAB also caused the H−L_W−V equilibrium conditions to be shifted to the stabilized region represented by higher temperature and lower pressure conditions when compared with those of the pure CO_2 hydrate.

In the present study, a ^{13}C MAS NMR experiment was carried out to analyze the CH_4 + TBAB semiclathrates because NMR spectroscopy has been recognized as a powerful tool for the structure identification and composition analysis of clathrates.[28]

Table 1. Semiclathrate Phase Equilibrium Data for the CH_4 + TBAB + Water Systems

0.6 mol %		3.7 mol %		7.7 mol %	
T (K)	P (MPa)	T (K)	P (MPa)	T (K)	P (MPa)
286.35 ± 0.05	2.23 ± 0.01	288.75 ± 0.05	2.08 ± 0.01	287.35 ± 0.05	2.45 ± 0.01
288.10 ± 0.10	3.58 ± 0.01	290.55 ± 0.05	3.52 ± 0.01	288.75 ± 0.05	3.69 ± 0.01
289.55 ± 0.05	5.32 ± 0.02	292.00 ± 0.10	5.28 ± 0.01	290.30 ± 0.10	5.26 ± 0.01
290.75 ± 0.05	7.09 ± 0.01	292.95 ± 0.05	6.80 ± 0.01	291.35 ± 0.05	7.20 ± 0.02
291.45 ± 0.05	8.87 ± 0.01	294.15 ± 0.05	9.01 ± 0.01	292.25 ± 0.05	9.17 ± 0.01

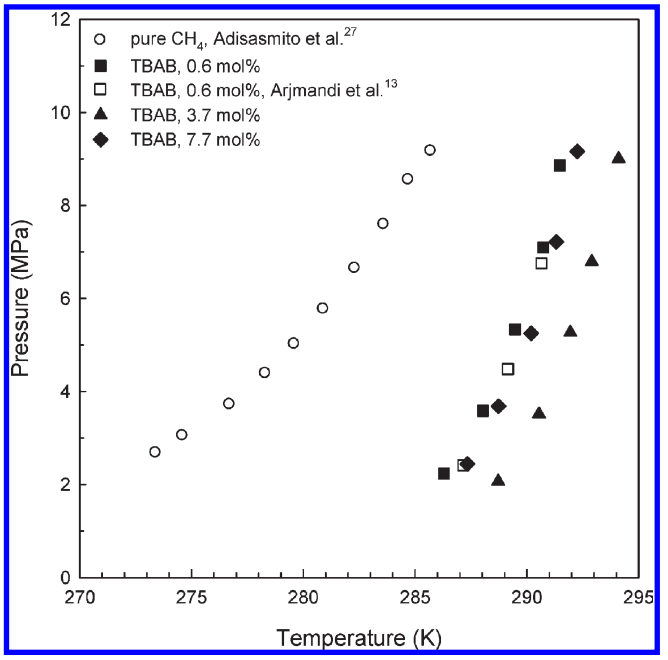

Figure 3. Semiclathrate phase equilibria of the CH_4 + TBAB + water systems.

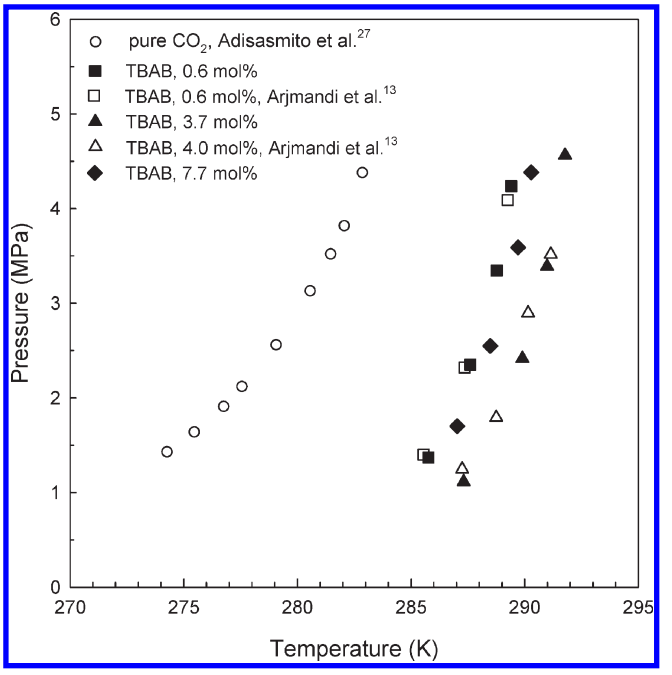

Figure 4. Semiclathrate phase equilibria of the CO_2 + TBAB + water systems.

Shimada et al.[5] indicated through X-ray diffraction (XRD) that in pure TBAB semiclathrate TBA^+ is located at the center of four partially broken cages whereas the dodecahedral cages (5^{12}) are empty. However, in the double CH_4 + TBAB semiclathrate CH_4 gas enclathration has not yet been confirmed via NMR even though the cage-dependent ^{13}C NMR chemical shifts for the enclathrated guest molecules can be used to determine structure types of the formed clathrates.[21,22,28] Figure 5 shows a stacked plot of the ^{13}C MAS NMR spectra of pure TBAB (3.7 mol %) semiclathrate, double CH_4 + TBAB (3.7 mol %) semiclathrate, and CH_4 hydrate. The spectrum of the CH_4 hydrate, known to form structure I (sI), has two resonance peaks at −4.3 and −6.6 ppm. The peak at −4.3 ppm can be assigned to CH_4 molecules in the small 5^{12} cages and the peak at −6.6 ppm to CH_4 molecules in the large $5^{12}6^2$ cages, considering the ideal stoichiometric ratio of the small 5^{12} to the large $5^{12}6^2$ cages in the unit cell of sI. On the other hand, pure TBAB (3.7 mol %) semiclathrate showed four resonance peaks at 58.8, 24.4, 20.3, and 14.3 ppm, which can be assigned to four carbons of the *n*-butyl group of TBAB. The double CH_4 + TBAB (3.7 mol %) semiclathrate also showed four resonance peaks at 58.8, 24.4, 20.3, and 14.3 ppm, which are the same as those from the *n*-butyl group of pure TBAB semiclathrate. In addition, the double CH_4 + TBAB (3.7 mol %) semiclathrate additionally demonstrated one resonance peak at −4.3 ppm, which is the same as that from CH_4 molecules in the small 5^{12} cages of CH_4 hydrate. Accordingly, the additional resonance peak at −4.3 ppm can be assigned to CH_4 molecules captured in the 5^{12} cages of the double semiclathrate. Figure 6 shows a stacked plot of the ^{13}C MAS NMR spectra of pure TBAB (0.6 mol %) semiclathrate, double CH_4 + TBAB (0.6 mol %) semiclathrate, and CH_4 hydrate. The positions of resonance peaks from the *n*-butyl group of both pure TBAB (0.6 mol %) and double CH_4 + TBAB (0.6 mol %) semiclathrates were the same as those of both pure TBAB (3.7 mol %) and double CH_4 + TBAB (3.7 mol %) semiclathrates. Furthermore, the position of the resonance peak from CH_4 molecules captured in the double CH_4 + TBAB (0.6 mol %) semiclathrate was also the same as that in the CH_4 hydrate. We could not find any chemical shift discrepancy of the *n*-butyl group between pure and double semiclathrates. However, accurate cage occupancy for CH_4 molecules in the double semiclathrates could not be obtained because resonance peaks from the *n*-butyl group of TBAB were not clearly separated and, thus, it is difficult to calculate the relative integrated areas. From the chemical shifts of ^{13}C NMR spectra, it is concluded that CH_4 molecules are captured in the 5^{12} cages of the double CH_4 + TBAB semiclathrate and enclathration of CH_4 does not change the structure of the semiclathrate.

Table 2. Semiclathrate Phase Equilibrium Data for the CO_2 + TBAB + Water Systems

0.6 mol %		3.7 mol %		7.7 mol %	
T (K)	P (MPa)	T (K)	P (MPa)	T (K)	P (MPa)
285.70 ± 0.10	1.35 ± 0.02	287.35 ± 0.05	1.12 ± 0.01	287.05 ± 0.05	1.72 ± 0.02
287.55 ± 0.05	2.34 ± 0.01	290.00 ± 0.10	2.43 ± 0.01	288.40 ± 0.10	2.53 ± 0.02
288.70 ± 0.10	3.34 ± 0.01	290.95 ± 0.05	3.38 ± 0.01	289.75 ± 0.05	3.60 ± 0.01
289.45 ± 0.05	4.25 ± 0.01	291.75 ± 0.05	4.55 ± 0.01	290.20 ± 0.01	4.37 ± 0.01

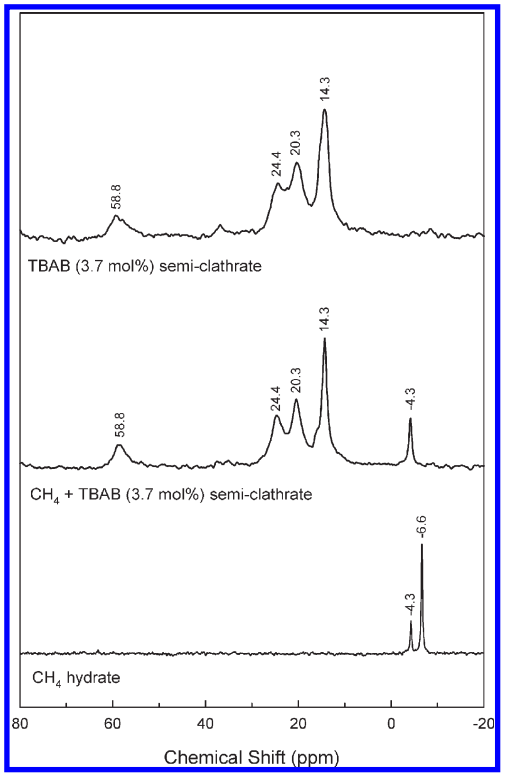

Figure 5. ^{13}C NMR spectra of pure TBAB (3.7 mol %) semiclathrate (0.1 MPa and 275.15 K), double CH_4 + TBAB (3.7 mol %) semiclathrate (8.0 MPa and 285.15 K), and CH_4 hydrate (8.0 MPa and 274.15 K). Pressure and temperature values in parentheses are sample preparation conditions of each semiclathrate and hydrate.

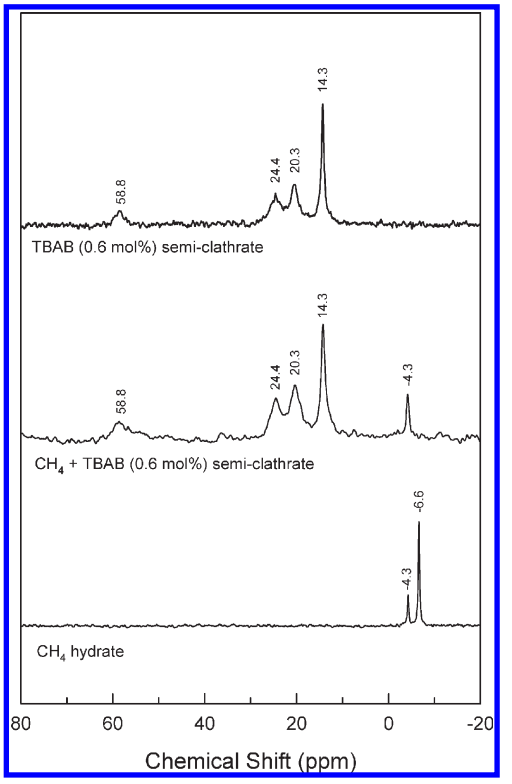

Figure 6. ^{13}C NMR spectra of pure TBAB (0.6 mol %) semiclathrate (0.1 MPa and 275.15 K), double CH_4 + TBAB (0.6 mol %) semiclathrate (8.0 MPa and 285.15 K), and CH_4 hydrate (8.0 MPa and 274.15 K). Pressure and temperature values in parentheses are sample preparation conditions of each semiclathrate and hydrate.

Raman spectroscopy, known to be simpler and less resource intensive,[29] was also used to investigate guest gas enclathration and the structural aspect of the semiclathrates. The Raman spectrum of pure CO_2 gas consists of two major bands called the Fermi dyad and two minor bands that are coupled through Fermi resonance.[30] When CO_2 molecules are incorporated into the gas hydrate lattice of sI, the major bands are still quite noticeable, but the minor bands are merged into the Fermi dyad bands, as shown in Figure 7. The Raman spectrum for pure CO_2 hydrate does not show peak splittings even though CO_2 molecules occupy both the small and large cages of sI.[31] To examine the wavenumber shift due to the structure transition, the Raman spectrum of CO_2 + THF (5.6 mol %) hydrate, known to form structure II (sII), is also depicted in Figure 7. The overall shape of the peaks appeared to be almost the same as that of pure CO_2 hydrate. The structural transition of sI to sII by the inclusion of THF into the mixed hydrate resulted in a wavenumber shift of a small peak (1276 $cm^{-1} \rightarrow$ 1274 cm^{-1}), but the wavenumber of a large peak of sII was found at almost the same position as that of sI. For CO_2 + TBAB semiclathrates, peaks from CO_2 molecules enclathrated in the double semiclathrates were shown at 1273 and 1380 cm^{-1} even though many peaks from TBAB appeared at a wide range of wavenumbers. In addition, it is possible to distinguish the crystal structures (type A and type B) of the semiclathrates from the Raman spectra. As indicated by Hashimoto et al.,[8] the peaks around 1100 and 1400 cm^{-1} of the semiclathrates were affected by the crystal structures. From the Raman spectra, CO_2 enclathration in the double TBAB semiclathrate was confirmed and a slight peak shift due to the structure transition was detected. However, the accurate information on cage occupancy for CO_2 could not be obtained because, unlike ^{13}C NMR spectra, the Raman spectra for CO_2 hydrate did not show any peak splittings for guests in different cages. More investigation on structure details and accurate guest

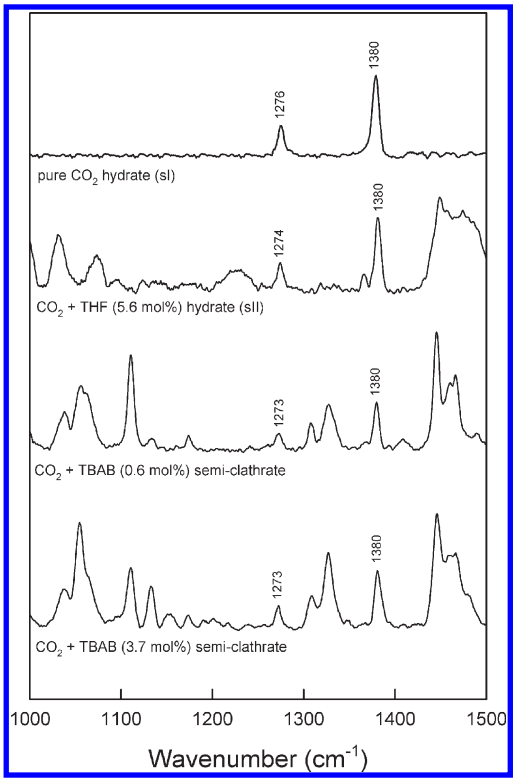

Figure 7. Raman spectra of pure CO_2 hydrate (3.5 MPa and 274.15 K), mixed CO_2 + THF hydrate (3.5 MPa and 282.65 K), and double CO_2 + TBAB semiclathrates (3.5 MPa and 282.65 K). Pressure and temperature values in parentheses are sample preparation conditions of each semiclathrate and hydrate.

gas behavior of the CO_2 + TBAB semiclathrates should be achieved in the near future through more sophisticated analysis methods.

CONCLUSIONS

The three-phase ($H-L_W-V$) clathrate equilibria of TBAB semiclathrates were measured using two different types of guest gases (CH_4 and CO_2). The presence of TBAB greatly stabilized the double semiclathrates and, accordingly, caused the $H-L_W-V$ equilibrium line of the double semiclathrates to be greatly shifted to the higher temperature and lower pressure regions when compared to that of pure gas hydrate. As can be expected from the temperature−composition relation of pure TBAB semiclathrates, the highest stabilization effect in the double semiclathrates was observed at the stoichiometric concentrations corresponding to the hydration number of pure TBAB semiclathrate, which is 3.7 mol %. At a concentration over stoichiometry, the excess amount of TBAB can inhibit semiclathrate formation. The dissociation temperature and dissociation enthalpy of pure TBAB semiclathrate were also confirmed by DSC. The NMR and Raman spectroscopic studies identified the enclathration of guest gases (CH_4 and CO_2) in the double semiclathrates. In particular, from the cage-dependent ^{13}C NMR chemical shift, it was confirmed that CH_4 molecules were captured in the 5^{12} cages of the double semiclathrates and CH_4 enclathration did not affect the structure of the semiclathrate. The overall thermodynamic and spectroscopic results obtained in this study can be used for understanding the fundamental guest gas behavior of the double semiclathrates and, thus, could be applied as valuable information in gas storage and separation using semiclathrates.

ASSOCIATED CONTENT

Supporting Information. All the original experimental data in Figures 1, 3, and 4. This material is available free of charge via the Internet at http://pubs.acs.org.

AUTHOR INFORMATION

Corresponding Author

*Phone: 82-55-213-3757. Fax: 82-55-283-6465. E-mail: yseo@changwon.ac.kr.

ACKNOWLEDGMENT

This work was supported by the Energy Efficiency & Resources Program and Human Resources Development Program of the Korea Institute of Energy Technology Evaluation and Planning (KETEP) and by the Basic Research Project of the Korea Institute of Geoscience and Mineral Resources (KIGAM) funded by the Ministry of Knowledge Economy of Korea. This work was also supported by the Basic Science Research Program through the National Research Foundation of Korea (NRF) funded by the Ministry of Education, Science and Technology (Grant 2009-0069569). We thank Mr. I. S. Joo (Center for Research Facilities, Changwon National University) for his support with respect to DSC and Raman measurements.

REFERENCES

(1) Sloan, E. D.; Koh, C. A. *Clathrate Hydrates of Natural Gases*, 3rd ed.; CRC Press: Boca Raton, FL, 2008.
(2) McMullan, R.; Jeffrey, G. A. *J. Chem. Phys.* **1959**, *31*, 1231–1234.
(3) Dyadin, Y. A.; Bondaryuk, I. V.; Aladko, L. S. *J. Struct. Chem.* **1995**, *36*, 995–1045.
(4) Aladko, L. S.; Dyadin, Y. A.; Rodionova, T. V.; Terekhova, I. S. *J. Struct. Chem.* **2002**, *43*, 990–994.
(5) Shimada, W.; Shiro, M.; Kondo, H.; Takeya, S.; Oyama, H.; Ebinuma, T.; Narita, H. *Acta Crystallogr.* **2005**, *C61*, o65–o66.
(6) Chapoy, A.; Anderson, R.; Tohidi, B. *J. Am. Chem. Soc.* **2007**, *129*, 746–747.
(7) Hashimoto, S.; Murayama, S.; Sugahara, T.; Sato, H.; Ohgaki, K. *Chem. Eng. Sci.* **2006**, *61*, 7884–7888.
(8) Hashimoto, S.; Sugahara, T.; Moritoki, M.; Sato, H.; Ohgaki, K. *Chem. Eng. Sci.* **2008**, *63*, 1092–1097.
(9) Kamata, Y.; Oyama, H.; Shimada, W.; Ebinuma, T.; Takeya, S.; Uchida, T.; Nagao, J.; Narita, H. *Jpn. J. Appl. Phys.* **2004**, *43*, 362–365.
(10) Duc, N. H.; Chauvy, F.; Herri, J. H. *Energy Convers. Manage.* **2007**, *48*, 1313–1322.
(11) Fan, S.; Li, S.; Wang, J.; Lang, X.; Wang, Y. *Energy Fuels* **2009**, *23*, 4202–4208.
(12) Li, D. L.; Du, J. W.; Fan, S. S.; Liang, D. Q.; Li, X. S.; Huang, N. S. *J. Chem. Eng. Data* **2007**, *52*, 1916–1918.
(13) Arjmandi, M.; Chapoy, A.; Tohidi, B. *J. Chem. Eng. Data* **2007**, *52*, 2153–2158.
(14) Mohammadi, A. H.; Richon, D. *J. Chem. Eng. Data* **2010**, *55* 982–984.
(15) Li, S.; Fan, S.; Wang, J.; Lang, X.; Wang, Y. *J. Chem. Eng. Data* **2010**, *55*, 3312–3315.
(16) Sun, Z. G.; Sun, L. *J. Chem. Eng. Data* **2010**, *55*, 3538–3541.
(17) Seo, Y.; Lee, H. *Environ. Sci. Technol.* **2001**, *35*, 3386–3390.
(18) Seo, Y.; Lee, S.; Cha, I.; Lee, J. D.; Lee, H. *J. Phys. Chem. B* **2009**, *113*, 5487–5492.

(19) Cha, I.; Lee, S.; Lee, J. D.; Lee, G. W.; Seo, Y. *Environ. Sci. Technol.* **2010**, *44*, 6117–6122.
(20) Seo, Y.; Lee, H. *J. Phys. Chem. B* **2002**, *106*, 9668–9673.
(21) Lee, S.; Cha, I.; Seo, Y. *J. Phys. Chem. B* **2010**, *114*, 15079–15084.
(22) Lee, S.; Seo, Y. *Langmuir* **2010**, *26*, 9742–9748.
(23) Lipkowski, J.; Komarov, V. Y.; Rodionova, T.; Dyadin, Y. A.; Aladko, L. S. *J. Supramol. Chem.* **2002**, *2*, 435–439.
(24) Oyama, H.; Shimada, W.; Ebinuma, T.; Kamata, Y.; Takeya, S.; Uchida, T.; Nagao, J.; Narita, H. *Fluid Phase Equilib.* **2005**, *234*, 131–135.
(25) Zhang, J. S.; Lee, J. W. *J. Chem. Eng. Data* **2009**, *54*, 659–661.
(26) Deschamps, J.; Dalmazzone, D. *J. Therm. Anal. Calorim.* **2009**, *98*, 113–118.
(27) Adisasmito, S.; Frank, R. J.; Sloan, E. D. *J. Chem. Eng. Data* **1991**, *36*, 68–71.
(28) Ripmeester, J. A.; Ratcliffe, C. I. *J. Struct. Chem.* **1999**, *40* 654–662.
(29) Uchida, T.; Hirano, T.; Ebinuma, T.; Narita, H.; Gohara, K.; Mae, S.; Matsumoto, R. *AIChE J.* **1999**, *45*, 2641–2645.
(30) Sum, A. K.; Burruss, R. C.; Sloan, E. D. *J. Phys. Chem. B* **1997**, *101*, 7371–7377.
(31) Udachin, K. A.; Ratcliffe, C. I.; Ripmeester, J. A. *J. Phys. Chem. B* **2001**, *105*, 4200–4204.